

## THE DETERMINATION OF $\sigma^{\text{had}}$ WITH THE KLOE DETECTOR\*

STEFAN E. MÜLLER

For the KLOE Collaboration

Laboratori Nazionali di Frascati  
Via E. Fermi 40, 00044 Frascati (RM), Italy

*(Received June 28, 2007)*

Using the radiative return allows for precision measurements of energy-dependent cross sections at particle factories. In the first part, the method of the measurement and its application at the KLOE experiment will be explained. In the second part, the status of the ongoing analyses based on the 2002 data set is presented. These analyses will improve the published result in many aspects and allow for important cross checks.

PACS numbers: 13.40.Gp, 13.60.Hb, 13.66.Bc, 13.66.De

### 1. Introduction

The hadronic contribution to the muon anomaly  $a_\mu = (g_\mu - 2)/2$  can be related to the hadronic cross sections via a dispersion relation

$$a_\mu^{\text{hadr}} = \frac{1}{4\pi^3} \int_{4m_\pi^2}^{\infty} \sigma_{e^+e^- \rightarrow \text{hadr}}(s) K(s) ds, \quad (1)$$

where the integral is carried out over the invariant mass squared  $s$  of the hadronic system and the kernel  $K(s)$  behaves approximately like  $1/s$ . The annihilation cross section is largely enhanced around the mass of the  $\rho$  meson. Data at low energies contribute therefore strongly to  $a_\mu^{\text{hadr}}$ . Since perturbative QCD fails at energies below  $\sim 2.5$  GeV, there one has to use experimentally measured cross sections in the dispersion integral. Their experimental uncertainty is dominating the theoretical evaluation of  $a_\mu$ . In

---

\* Presented at The Final EURIDICE Meeting “Effective Theories of Colours and Flavours: from EURODAPHNE to EURIDICE”, Kazimierz, Poland, 24–27 August, 2006.

particular, the  $2\pi$ -channel contributes about 70% to the uncertainty of  $a_\mu^{\text{hadr}}$ . The current theoretical and experimental status of  $a_\mu$  has been reviewed in [1] and [2]. Confronting recent theoretical evaluations of  $a_\mu$  (including cross section data from CMD2 [3, 4], KLOE [5] and SND [6]) with the final experimental result by the E821 experiment [7], one finds a  $\sim 3\sigma$  deviation. To improve the significance of this deviation, precise measurements of hadronic cross sections at low energies are needed. In addition, a precision at a 1% level on hadronic cross sections up to energies of  $\sim 10$  GeV is required for a precise determination of  $\alpha_{\text{em}}(s)$  as needed for physics at a future linear  $e^+e^-$  collider [8].

## 2. Measuring $\sigma_{\pi\pi\gamma(\gamma)}$ with the KLOE detector

The standard way to measure hadronic cross sections in the past was to perform an energy scan, in which the energy of the colliding beams was changed to the desired value. As this is not desirable at the Frascati  $e^+e^-$  collider DAΦNE, which was designed to operate at the fixed energy of the  $\phi$  resonance (1019.5 MeV) with high luminosity [9], one exploits the photonic *radiative return* to measure cross sections below the fixed energy [10, 11]. In this process, the collision energy is lowered because one or more photon(s) radiate off the electron or positron in the initial state. Thus the cross sections become accessible from the  $\phi$  mass down to the production threshold of the particles in the final state. The hadronic cross section  $\sigma(e^+e^- \rightarrow \text{hadrons})$  can be obtained by measuring the differential cross section  $d\sigma(e^+e^- \rightarrow \text{hadr} + \gamma_{\text{ISR}}(\gamma))/ds'$ , where  $s' = M_{\text{hadr}}^2$  after initial state radiation. Neglecting for the moment the presence of photons from final state radiation, one can relate the two quantities by the radiation function  $H$ :

$$\frac{d\sigma(\text{hadrons} + \gamma(\gamma)_{\text{ISR}})}{ds'} s' = \sigma(\text{hadrons}) \times H(s'). \quad (2)$$

As the obtained cross section to be put into the dispersion integral has to be inclusive with respect to photons from final state radiation, their contribution to the observed signal has to be estimated very carefully. An indispensable tool for the analyses are thus Monte Carlo generators describing both the effects from initial state radiation (the  $H$ -function in Eq. 2) and final state radiation. The analyses done at the KLOE-experiment have especially profited from the PHOKHARA generator, which contains the description of initial and final state radiation at next-to-leading order [12–14]. An effort to describe pionic final state radiation beyond the point-like pions approximation has been done in [15], see also [16].

## 2.1. Signal selection

The KLOE detector (Fig. 1, (left)) consists of a high resolution drift chamber ( $\sigma_p/p \leq 0.4\%$ ) [17] and an electromagnetic calorimeter ( $\sigma_t \sim 57 \text{ ps}/\sqrt{E [\text{GeV}]} \oplus 100 \text{ ps}$ ) [18]. The final state to be searched for is composed of two charged pions and one or more photons. Two different selection regions are considered: In the *small angle* analysis photons are emitted within a cone of  $\theta_\gamma < 15^\circ$  around the beamline (narrow cones in Fig. 1, (left)), while in the *large angle* analysis there should be at least one photon at a polar angle of  $50^\circ < \theta_\gamma < 130^\circ$  (large central cones in Fig. 1, (left)). In both cases the two charged pion tracks should have  $50^\circ < \theta_\pi < 130^\circ$ .

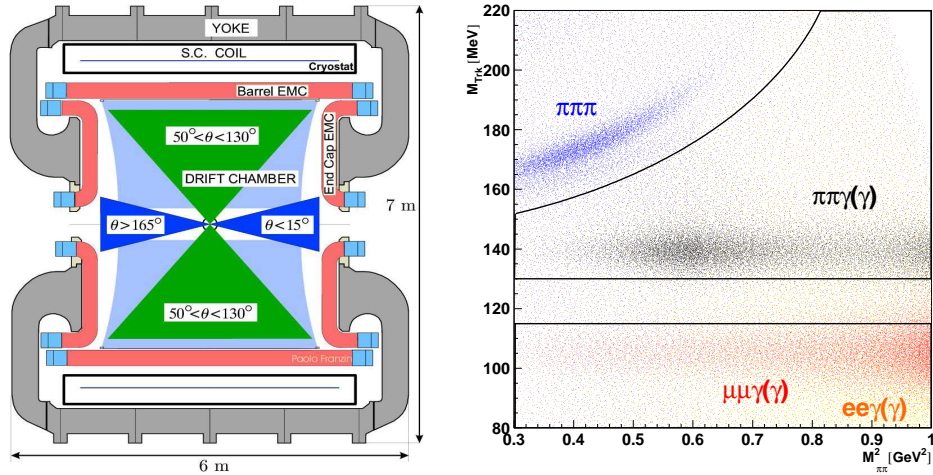


Fig. 1. Left: KLOE detector with the selection regions for the small angle photons (narrow cones) and for pion tracks and large angle photons (wide cones). Right: Signal and background distributions in the  $M_{\text{Trk}} - M_{\pi\pi}^2$ -plane. Two possible selection scenarios are shown — for pions (upper area) and for muons (lower area).

The photon is not explicitly detected in the *small angle* analysis, its direction is reconstructed from the tracks' directions by closing kinematics:  $\vec{p}_\gamma = -(\vec{p}_{\pi^+} + \vec{p}_{\pi^-})$ . The separation of pion- and photon selection regions in this analysis greatly reduces the contamination from the resonant process  $e^+e^- \rightarrow \phi \rightarrow \pi^+\pi^-\pi^0$  in which the  $\pi^0$  mimicks the missing momentum of the photon(s) and from the final state radiation process  $e^+e^- \rightarrow \pi^+\pi^-\gamma_{\text{FSR}}$ . Since ISR-photons are mostly collinear with the beam line, a high statistics for the ISR signal events remains. On the other hand, a highly energetic photon emitted at small angle forces the pions also to be at small angles (and thus outside the selection cuts), resulting in a kinematical suppression of events with  $M_{\pi\pi}^2 < 0.35 \text{ GeV}^2$ . This is not the case for the *large angle* analysis, which allows us to measure the spectrum down to the 2-pion threshold

of  $4m_\pi^2$ . The price to pay in the *large angle* analysis is an increased contribution from irreducible, model-dependent background processes such as events with final state radiation and the decay  $\phi \rightarrow f_0\gamma \rightarrow \pi^+\pi^-\gamma$ , whose effects have to be estimated from Monte Carlo simulations. To further clean up the samples from reducible background like  $\phi \rightarrow \pi^+\pi^-\pi^0$ ,  $e^+e^- \rightarrow e^+e^-\gamma$  and  $e^+e^- \rightarrow \mu^+\mu^-\gamma$ , cuts in kinematical variables named *trackmass*<sup>1</sup> and *missing mass*<sup>2</sup>, are used (see Fig. 1, (right)). A particle ID estimator based on calorimeter information and time-of-flight is used to suppress the huge cross section for radiative Bhabhas. From the spectrum of observed events, the differential cross section is obtained via

$$\frac{d\sigma(\pi\pi\gamma(\gamma))}{ds'} = \frac{\Delta N_{\text{Obs}} - \Delta N_{\text{Bkg}}}{\Delta M_{\pi\pi}^2} \frac{1}{\varepsilon_{\text{Sel}}} \frac{1}{\int L dt}. \quad (3)$$

### 2.2. Background evaluation

The contribution from background is evaluated using a fit of Monte Carlo simulated distributions for signal together with background channels to the observed data spectrum. Great care has to be taken in order to ensure that the Monte Carlo distributions match the data as closely as possible. At KLOE, the Monte Carlo simulations follow the data taking conditions (exact  $\sqrt{s}$ , machine background level) on a run-by-run basis. Resolutions of the detector components have been evaluated from data and are included in the detector simulation [19]. From the normalisation parameters of the background channels obtained from the fit one can deduce the contamination of the data spectrum. Fig. 2, (left), shows an example of fitting the trackmass distribution of data with MC distributions from  $\mu\mu\gamma(\gamma)$  and  $\pi\pi\gamma(\gamma)$ .

### 2.3. Efficiencies

Efficiencies have to be evaluated for each selection step as a function (or in bins) of  $M_{\pi\pi}^2$ . They are defined as  $\varepsilon_{\text{Signal}} = N_{\text{Sel,Signal}}/N_{\text{In}}$ . Ideally,  $\varepsilon_{\text{Signal}}$  of a selection step should be much higher than  $\varepsilon_{\text{Bkg}}$  in order to enhance the signal in the selection. A difficulty consists in evaluating the efficiency on the signal events, since the sample of selected events contains both signal and a fraction of background events. Common ways to overcome the problem include the use of independently selected control samples, exploiting the information from downscaled events retained during the data taking, or evaluating the efficiencies from the Monte Carlo simulation after having

<sup>1</sup> Defined under the hypothesis that the final state consists of two charged particles with equal mass  $m_{\text{trk}}$  and one photon.

<sup>2</sup> Defined as  $m_{\text{miss}} = \sqrt{E_X^2 - |\vec{P}_X|^2}$  assuming that the underlying process is  $e^+e^- \rightarrow \pi^+\pi^-X$ . It is peaked at the  $\pi^0$  mass for  $\pi^+\pi^-\pi^0$  events.

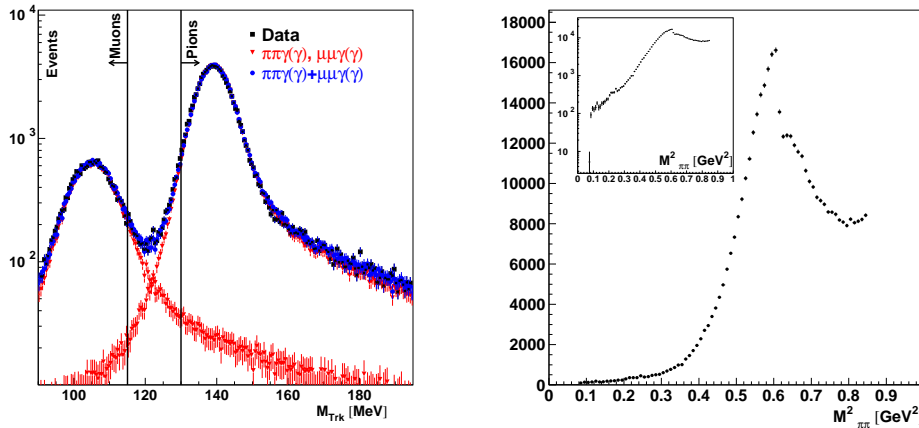


Fig. 2. Left: Example of fitting the trackmass distribution of data with MC distributions from  $\mu\mu\gamma(\gamma)$  and  $\pi\pi\gamma(\gamma)$  for  $0.72 < M_{\pi\pi}^2 < 0.74 \text{ GeV}^2$ . Right: Preliminary spectrum from 2002 data for the large angle analysis.

verified that Monte Carlo describes the detector conditions with adequate accuracy. In order to obtain a precision of 1% or better on  $\sigma_{\pi\pi}$ , efficiencies have to be evaluated with permil precision as a function of  $M_{\pi\pi}^2$ .

#### 2.4. Luminosity

At KLOE, luminosity is measured using Bhabha events at large angles ( $55^\circ < \theta < 125^\circ$ ). The effective cross section of  $\sim 430 \text{ nb}$  ensures sufficient statistics. Two independent generators are used to calculate the reference process: The BABAYAGA generator [20] and the BHAGENF generator [21, 22]. Both generators agree very well with each other in terms of cross section and differential distributions. The quoted error in both cases is 0.5%, giving (together with the experimental uncertainty of 0.3%) an uncertainty on the luminosity measurement of 0.6%. A detailed description of the luminosity measurement at KLOE can be found in [23].

#### 2.5. Final state radiation

Events with final state radiation can not be distinguished from the signal ISR events in the detector. The effect of final state radiation is to shift the measured invariant mass of the 2-pion-system away from the invariant mass of the virtual photon. This results in a small distortion of the spectrum, which has to be corrected by estimating the effect from Monte Carlo simulations. Especially leading-order final state radiation, in which the  $e^+e^-$  col-

lide at the energy of  $m_\phi$  without emitting an ISR-photon, creates a large tail of events at high  $M_{\pi\pi}^2$ . These events should not be considered in the analysis (in order to avoid the region with soft ISR-photon emission, the signal region is limited to events below  $\sim 0.95 \text{ GeV}^2$ ) and their contribution is subtracted from the spectrum. For the *small angle* cuts, this contribution is well below 0.5% since the FSR-photons are emitted preferably in the direction of the pions and not at small angle. For the *large angle* photon cuts, the contribution reaches up to 20% above and below the region of the  $\rho$ -meson. Another effect which has to be considered is the events with simultaneous emission of one photon in the initial state and one photon in the final state (next-to-leading order FSR) which are cut out by the  $\pi\pi\pi$ -suppressing elliptical cut in Fig. 1, (right). These events have to be added back to the spectrum to be fully inclusive in FSR in the desired energy range. Also this is done by evaluating their contribution with Monte Carlo simulations.

### 3. Results and new approaches

KLOE has successfully applied the radiative return to the measurement of the  $2\pi$ -cross section using the *small angle* analysis cuts on  $140 \text{ pb}^{-1}$  of 2001 data [5]. Putting this result in Eq. (1) to evaluate  $a_\mu^{\pi\pi}$  between 0.35 and  $0.95 \text{ GeV}^2$ , one obtains  $a_\mu^{\pi\pi} = (388.7 \pm 0.8_{\text{stat}}) \times 10^{-10}$  with a systematic error of  $\delta_{\text{sys}}(a_\mu^{\pi\pi})/a_\mu^{\pi\pi} = 0.9\%_{\text{exp}} \oplus 0.9\%_{\text{th}} = 1.3\%_{\text{tot}}$ . To push the total systematic error below 1%, a new analysis is carried out with small angle photon cuts using  $240 \text{ pb}^{-1}$  of 2002 data which have less machine background and improved calibration conditions. Together with modifications on trigger and offline software, these alone should allow to reach the desired accuracy. In addition, one can try to extract  $|F_\pi|^2$  from the ratio of observed pion and muon cross sections. Effects like luminosity and radiator function and their uncertainties should cancel out in the ratio. This requires however a precise selection of muon events. In the analysis, muons are separated from pions by a cut in the trackmass variable (see Fig. 1, (right) and Fig. 2, (left)). A comparison of the muon yield with the Monte Carlo expectation allows a cross check of the radiative corrections in the Monte Carlo. To extend the measurement towards the production threshold, a complementary analysis using photons at large angles is under way. In this analysis, based on the 2002 data, the photon can be detected and the closure of kinematics can be used to suppress background. Fig. 2, (right), shows the preliminary spectrum for this analysis. The main limitation is caused by the contribution from model dependent effects of  $\phi$ -decays ( $\phi \rightarrow f_0\gamma, \phi \rightarrow \rho\pi$  with  $\rho^\pm \rightarrow \pi^\mp\gamma$ ) and final state radiation.

#### 4. Conclusions

The KLOE experiment has proven the feasibility of using the *radiative return* to make precision cross section measurements at meson factories, and has published a first result for  $\sigma_{\pi\pi}$  based on 2001 data. New analyses are in progress using the 2002 data to improve and cross-check the result. In addition, the  $2 \text{ fb}^{-1}$  from 2004–05 data taking, plus the data taken off-resonance at an energy of 1 GeV, will allow for further improvements on the measurement in the future.

#### REFERENCES

- [1] F. Jegerlehner, *Acta Phys. Pol. B* **38**, 3021 (2007), these proceedings.
- [2] S. Eidelman, *Acta Phys. Pol. B* **38**, 3015 (2007), these proceedings
- [3] R.R. Akhmetshin *et al.* [CMD2 Collaboration], *J. Exp. Theor. Phys. Lett.* **84**, 413 (2006).
- [4] R.R. Akhmetshin *et al.* [CMD2 Collaboration], *Phys. Lett.* **B648**, 28 (2007) [[hep-ex/0610021](#)].
- [5] A. Aloisio *et al.* [KLOE Collaboration], *Phys. Lett.* **B606**, 12 (2005).
- [6] M.N. Achasov *et al.* [SND Collaboration], *Zh. Eksp. Teor. Fiz.* **130**, 437 (2006).
- [7] G.W. Bennett *et al.* [Muon g-2 Collaboration], *Phys. Rev.* **D73**, 072003 (2006).
- [8] F. Jegerlehner, *Nucl. Phys. B (Proc. Suppl.)* **162**, 22 (2006).
- [9] C. Bloise, *Acta Phys. Pol. B* **38**, 2731 (2007), these proceedings.
- [10] S. Binner, J.H. Kühn, K. Melnikov, *Phys. Lett.* **B459**, 279 (1999).
- [11] S. Spagnolo, *Eur. Phys. J.* **C6**, 637 (1999).
- [12] H. Czyż, A. Grzelińska, J. Kühn, G. Rodrigo, *Eur. Phys. J.* **C27**, 563 (2003).
- [13] H. Czyż, A. Grzelińska, J. Kühn, G. Rodrigo, *Eur. Phys. J.* **C33**, 333 (2004).
- [14] H. Czyż, A. Grzelińska, *Acta Phys. Pol. B* **38**, 2989 (2007), these proceedings.
- [15] G. Pancheri, O. Shekhovtsova, G. Venanzoni, *Phys. Lett.* **B642**, 342 (2006).
- [16] G. Pancheri, O. Shekhovtsova, G. Venanzoni, *Acta Phys. Pol. B* **38**, 2999 (2007), these proceedings.
- [17] M. Adinolfi *et al.* [KLOE Collaboration], *Nucl. Inst. Meth.* **A488**, 51 (2002).
- [18] M. Adinolfi *et al.* [KLOE Collaboration], *Nucl. Inst. Meth.* **A482**, 364 (2002).
- [19] F. Ambrosino *et al.* [KLOE Collaboration], *Nucl. Inst. Meth.* **A534**, 403 (2004).
- [20] C.M. Carloni Calame *et al.*, *Nucl. Phys.* **B584**, 459 (2000).
- [21] F. Berends, R. Kleiss, *Nucl. Phys.* **B228**, 537 (1983).
- [22] E. Drago, G. Venanzoni, INFN-Report INFN-AE-97-48 (1997).
- [23] F. Ambrosino *et al.* [KLOE Collaboration], *Eur. Phys. J.* **C47**, 589 (2006).